# Unveiling Optimal Operating Conditions for an Epoxy Polymerization Process Using Multi-objective Evolutionary Computation

Kalyanmoy Deb[1], Kishalay Mitra[2], Rinku Dewri[3], and Saptarshi Majumdar[4]

[1] Mechanical Engineering Department, Indian Institute of Technology Kanpur, Kanpur-208016, deb@iitk.ac.in, http://www.iitk.ac.in/kangal/deb.htm
[2] Manufacturing Practice, Tata Consultancy Services, 54B Hadapsar Industrial Estate, Pune-411013, India, kmitra@pune.tcs.co.in
[3] Department of Mathematics, Indian Institute of Technology Kharagpur, Kharagpur-721302, rinku@webteam.iitkgp.ernet.in
[4] Tata Research Development and Design Center, 54B Hadapsar Industrial Estate, Pune-411013, India, smajumdar@pune.tcs.co.in

**Abstract.** The optimization of the epoxy polymerization process involves a number of conflicting objectives and more than twenty decision parameters. In this paper, the problem is treated truly as a multi-objective optimization problem and near-Pareto-optimal solutions corresponding to two and three objectives are found using the elitist non-dominated sorting GA or NSGA-II. Objectives, such as the number average molecular weight, polydispersity index and reaction time, are considered. The first two objectives are related to productivity of the polymerization process. The decision variables are discrete addition quantities of various reactants e.g. the amount of addition for bisphenol-A (a monomer), sodium hydroxide and epichlorohydrin at different time steps, whereas the satisfaction of all species balance equations is treated as constraints. This study brings out a salient aspect of using an evolutionary approach to multi-objective problem solving. Important and useful patters of addition of reactants are unveiled for different optimal trade-off solutions. The systematic approach of multi-stage optimization adopted here for finding optimal operating conditions for epoxy polymerization process should further such studies on other chemical process and real-world optimization problems.

**Keywords:** Multi-objective optimization, genetic algorithms, real-world optimization, Pareto-optimal solutions, chemical engineering process optimization.

## 1 Introduction

Real-world optimization problems often demand to cater the need of solving more than one objective simultaneously. Multi-objective optimization problems lead to a set of optimal solutions, known as *Pareto-optimal* solutions, as opposed to the single solution provided by any single-objective optimization task.

Although only one solution must be chosen at the end of the optimization task and this often must be performed with the guidance of a decision maker, it is a better practice to first find a set of Pareto-optimal solutions to have an idea of the extent of trade-offs possible among the underlying objectives before focusing on a particular solution [7]. Although the field of research and application on multi-objective optimization is not new, the use of evolutionary multi-objective optimization (EMO) techniques in various engineering and business applications is a recent phenomenon. Polymerization processes, being quite complex in nature, offer themselves as an extremely challenging candidate for multi-objective optimization studies. In modeling the polymerization system, several molecular parameters, such as the number or weight average molecular weights ($M_n$ or $M_w$, respectively), the polydispersity index (PDI), concentration of different functional groups etc., can all be predicted quite accurately using various experimentally measured indices such as strength and stiffness of the final product. Moreover, the desired objectives in a polymerization process often exhibit conflicting relationships and therefore become an ideal problem for multi-objective optimization studies. In this paper, multi-objective optimization of a semibatch epoxy polymerization system which is often used to manufacture high-strength composites, reinforced plastics, adhesives, protective coatings in appliances, etc. is thoroughly investigated.

A recent review [2] reveals that several studies are carried out on multi-objective optimization of polymerization reactors. A number of studies [20, 10, 11, 3, 5] considered multi-objective optimization of copolymerization reactors. Wajge and Gupta [21] studied multi-objective optimization of the nylon-6 batch reactor and obtained different optimal temperature histories corresponding to different solutions on the Pareto-optimal set using the same technique. Sareen and Gupta [18] extended that work and studied the nylon-6 semibatch reactor and obtained different optimal pressure histories and optimal jacket fluid temperature corresponding to different solutions on the Pareto-optimal set. A number of studies using an EMO approach are carried out on the multi-objective optimization of nylon-6 and polymethyl methacrylate (PMMA) reactors [4, 16, 12, 13]. These studies are mainly based on adapted versions of the non-dominated sorting genetic algorithm (NSGA) developed by Srinivas and Deb [19].

In the Taffy process [14], the most popular industrial process for preparing epoxy polymers, bisphenol-A (monomer) and epichlorohydrin, in excess, are reacted in presence of sodium hydroxide (NaOH). Although it is well established that alkali plays a key role in the epoxy polymerization process, the role of addition of other reactants (bisphenol-A and epichlorohydrin) is not well established. Experimental and theoretical studies are very few in open literature for the epoxy polymerization process. Raha and Gupta (1998) used species balance and equation of moments approach to study the process. They gave special importance to build the entire modeling framework as well as the effect of kinetic parameters and reactant's effect over the performance of the reaction process. However, based on some earlier studies [17] which showed the importance of all three reactants, we launch the present detail study for a better understanding

of the true nature of interactions among three conflicting objectives associated in an epoxy polymerization process.

## 2 Problem Formulation

The complete kinetic scheme for the above mentioned polymerization system can be found elsewhere [1]. Raha, Majumdar and Gupta [17] have validated the model with available experimental data. Using the species balance approach, ODEs corresponding to the initial value problem (IVP) are derived for various species and their moments. The "state" of the reaction scheme can be well described by a set of 48 state variables ($\mathbf{x} = (x_1, x_2, \ldots, x_{48})^T$), including all species balance and moment balance equations:

$$\frac{\mathrm{d}x_i}{\mathrm{d}t} = f_i(\mathbf{x}, \mathbf{U}), \quad i = 1, 2, \ldots, 48, \tag{1}$$

where $\mathbf{x}$ and $\mathbf{U}$ are vectors of the state and manipulated variables (such as the amount of intermediate additions for different reactants at different times). Manipulated variable vector consists of three discrete histories, namely, discrete history for NaOH addition (described here with $U_1(t_j)$), discrete history for epichlorohydrin addition ($U_2(t_j)$) and discrete history for bisphenol-A addition ($U_3(t_j)$) (where $t_j$ is the $j$-th time of addition of reactants). Given three discrete profiles ($\mathbf{U}$ at time zero and at other time steps) and the initial conditions of all state variables ($\mathbf{x}$ at time zero), the reaction scheme model can be solved by using an explicit integrator (RK-type method) to solve all 48 differential equations. This simulation procedure can then be combined with NSGA-II [9] optimization code for performing a multi-objective optimization.

### 2.1 Defining the Optimization Problems

Three different multi-objective problems are studied here. The first problem (Problem 1) is related to the quality of polymer induced, whereas the second problem (Problem 2) addresses the productivity issue also:

$$\textbf{Problem 1}: \begin{cases} \text{Maximize } M_n \\ \text{Minimize PDI} \\ \text{subject to satisfying mass and moment balance equations,} \\ u_i^{min} \leq u_i \leq u_i^{max} \qquad i = 1, \ldots, 21. \end{cases} \tag{2}$$

One computer simulation runs from zero (initial condition, $t = 0$) to $t = t_{sim}$ (7 hr used here). Each of the three profiles ($U_1(t), U_2(t), U_3(t)$) are, therefore, discretized into seven equally spaced points. Each of these variables is forced to lie between a lower bound ($u_i^{min}$) and a upper ($u_i^{max}$) bound. No restriction on

the $M_n$ and PDI values are used as constraints, as the satisfaction of variable bounds will ensure limiting values on $M_n$ and PDI.

The objective for Problem 2 is a vector of two objective functions: maximization of $M_n$ and minimization of the overall reaction time, $t_{sim}$, subject to satisfying mass and moment balance equations. Here, the reaction time $t_{sim}$ is a decision variable, thereby making the total number of variables to 22.

The objective for Problem 3 is a vector of three objective functions: maximization of $M_n$, minimization of $t_{sim}$, and minimization of PDI, subject to mass and moment balance equations.

## 3 NSGA-II for the Epoxy Polymerization Problem

Each solution is represented as a real-valued vector of 21 (or 22 for problems 2 and 3) values indicating the addition of NaOH, EP, and $AA_0$. For the real-valued NSGA-II, we use the simulated binary crossover (SBX) and the polynomial mutation operators [8]. When a pre-specified maximum iteration count ($N = N_{max}$) is reached, NSGA-II is terminated and the non-dominated solutions of the final population are declared as the obtained Pareto-optimal solutions. In problems 1 and 2, $N_{max} = 200$ and a population size of $N_{pop} = 250$ are used. Since Problem 3 deals with a three-dimensional Pareto-optimal front, we have chosen a larger population size and run NSGA-II for more iterations: $N_{pop} = 1000$ and $N_{max} = 500$. The crossover and mutation probabilities are $p_c = 0.9$ and $p_m = 0.1$ are used for the real-coded NSGA-II. NSGA-II can handle mixed type of optimization problems. Thus, we have used the objectives as they are mentioned in the previous section.

Based on some earlier studies, following variable bounds are set here to allow the optimizer (NSGA-II) a substantial search space to look for the optimized solutions: (i) the addition of NaOH varies between 0.2 and 1.0 kmol/m$^3$ at $t = 0$ hr and between zero and 1.0 kmol/m$^3$ for $t > 0$ hr., (ii) the addition of EP varies between 0.2 and 2.0 kmol/m$^3$ at $t = 0$ hr and between zero and 2.0 kmol/m$^3$ for $t > 0$ hr., and (iii) the addition of $AA_0$ varies between 0.2 and 1.0 kmol/m$^3$ at $t = 0$ hr and between zero and 1.0 kmol/m$^3$ for $t > 0$ hr.

## 4 Discussion on Problem 1

A simulation result corresponding to the initial condition of Batzer and Zahir [1] (with $M_n = 633.2$ kg/kg-mole and PDI=1.61) is considered as the benchmark performance data with which our optimized solutions will be compared. The solutions termed as "Initial" in Figure 1 denote the objective vectors with which NSGA-II search process is started. The figure indicates that the random solutions (with the chosen variable bounds) are far from being close to the optimized front (marked as 'NSGA-II'), particularly producing solutions with large $M_n$ values. The figure clearly shows that a wide range of distribution in both $M_n$ and in PDI values are obtained. The trade-off obtained between the two objectives is also clear from the figure. The following observations can be made from the obtained

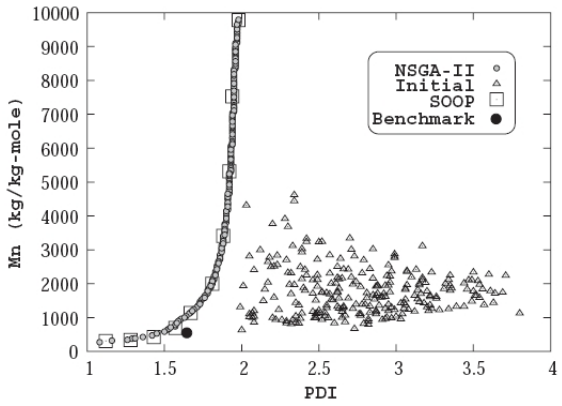


**Fig. 1.** Obtained NSGA-II solutions for the $M_n$ and PDI optimization are compared with single-objective optimization (SOOP) solutions. Initial solutions of NSGA-II and the benchmark solution are also shown.

results: (i) The resulting $M_n$-PDI trade-off is *non-convex*, a phenomenon which is rare in real-world multi-objective optimization problems, (ii) Investigating the solutions of Figure 1 further, it can be inferred that compared to the benchmark solution (marked as 'Benchmark' in the figure) there exist better solutions which can produce larger $M_n$ (ranging from 645 to 966 kg/kg-mole) and less PDI (ranging from 1.52 to 1.61, respectively) value, leading to polymers with better properties as compared to the benchmark solution.

In order to verify whether the obtained NSGA-II solutions are actually close to the true Pareto-optimal front of this problem, we use a single-objective preference based method next. Since, the above observation indicates that the Pareto-optimal front is non-convex, the commonly-used weighted-sum approach [15] may not be the right approach for this problem, as the the weighted-sum approach is known to be inadequate in finding the Pareto-optimal solutions in the non-convex region [6]. Thus, we use the $\epsilon$-constraint method [15] here. In this case, we convert the second objective (Minimization of PDI) into an additional constraint as PDI $\leq$ PDI$_\epsilon$ and maximize only the first objective. Other constraints and variable bounds, as given in Problem 1, are kept the same. To obtain different Pareto-optimal solutions, we simply choose a different value for PDI$_\epsilon$ and optimize the resulting single-objective optimization problem using a single-objective GA. The constraints are handled using a penalty parameter less procedure [6]. The GA parameters, such as the population size, operator parameters, etc., are kept the same as those used in the above NSGA-II study. Figure 1 marks these solutions as 'SOOP' solutions obtained by 10 independent GA runs, each performed with a different PDI$_\epsilon$ value. Since these solutions are found to lie on or near the Pareto-optimal front obtained by the NSGA-II, it can be stated that the non-dominated front found by NSGA-II is probably the true Pareto-optimal front.

### 4.1 Searching for Salient Properties of Pareto-Optimal Solutions

Each of the solutions on the Pareto-optimal front carries information about 21 decision variables. The Fritz-John necessary condition for Pareto-optimality conditions [6, 15] are presented below.

**Definition 1:** *(Fritz-John necessary condition). A necessary condition for* $\mathbf{x}^*$ *to be Pareto-optimal is that there exist vectors* $\gamma \geq \mathbf{0}$ *and* $\mathbf{v} \geq \mathbf{0}$ *(where* $\gamma \in \mathbb{R}^M$, $\mathbf{v} \in \mathbb{R}^J$ *and* $\gamma, \mathbf{v} \neq \mathbf{0}$*) such that the following conditions are true:*

*1)* $\sum_{m=1}^{M} \gamma_m \nabla f_m(\mathbf{x}^*) - \sum_{j=1}^{J} v_j \nabla g_j(\mathbf{x}^*) = \mathbf{0}$*, and*

*2)* $v_j g_j(\mathbf{x}^*) = 0$ *for all* $j = 1, 2, \ldots, J$,

where the underlying multi-objective optimization problem (with $M$ objectives $f_m$ to be minimized) is assumed to have $J$ inequality constraints: $g_j(\mathbf{x}) \geq 0$ for $j = 1, \ldots, J$. The above conditions, although cannot be applied to our problem directly due to the inability to compute the gradients of the objective functions and constraints, suggest certain common properties which all Pareto-solutions must satisfy. This leads us to believe that the obtained solutions, if close to the Pareto-optimal solutions, will share some common properties among them and, of course, will have some differences in order to have trade-offs among them. If such properties exist, they would be worth searching for in a real-world application problem, as the sheer knowledge of them will provide important and useful information about the optimal trade-off among objectives [7]. An investigation is performed next to identify whether the obtained $M_n$-PDI solutions bear any similarity in terms of associated decision variables. Interesting trends are discovered and shown in Figure 2.

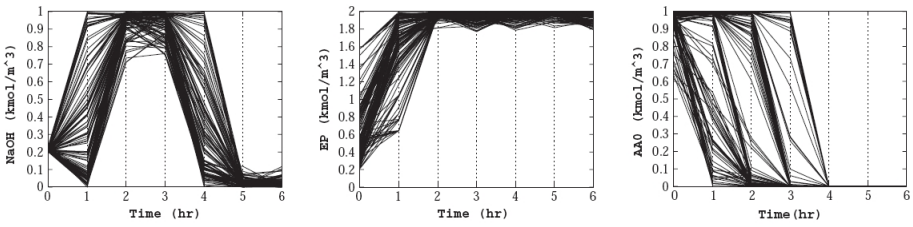


**Fig. 2.** Time-variant additions of NaOH (left), EP (center), and $AA_0$ (right) show common patterns for real-coded NSGA-II solutions on Problem 1.

Though the decision variables are discrete additions at various time steps, they are joined with straight lines to show trends. A casual look at the plots will reveal some interesting patterns followed in all obtained solutions. Although the additions at every hours could have been anywhere on the vertical axis at each time step, all obtained solutions seem to follow some patterns. These patterns reveal important insights about the optimal working characteristics of the epoxy

polymerization problem, some of which we have deciphered and are discussed in the following:

1) The general trend captured in NaOH addition is to start from the lower bound, reduce or increase the addition to the first hour, increase close to the upper bound in the next hour, then continue with the same amount for some more time and finally reduce close to the lower bound. A high amount of NaOH addition is required in the first phase of reaction process for a better initiation of polymerization and the amount of NaOH can be kept low in the later part of the process as mainly the growth of chain length occurs at that part of time and NaOH is produced as a by-product. The reason for NaOH to come down at the lower bound after addition at the zero-th hour for solutions is due to the fact that the initiation steps require NaOH as a reactant and also produce as a by-product. In case of $M_n$ value less than $7.0 \times 10^3$ kg/kg-mole, NaOH is found to be added to the system in a controlled fashion. For $M_n$ value greater than $7.0 \times 10^3$ kg/kg-mole, NaOH, instead of decreasing at time step of the first hour after the first addition, goes up and rest of the trend remains same as it is stated earlier. In these cases, NaOH takes part not only in the initiation but also in the growth of chain length by helping to form certain species of polymer ($BE_n$) which contributes significantly towards the high value of $M_n$.

2) The trend found for epichlorohydrin is straightforward. It must be started at different levels depending on the required $M_n$ value, but must be quickly increased close to the upper limit and must be continued at that amount till the end. The reason for small required value of epichlorohydrin initially is due to it having a less contribution in polymer chain initiation. However, epichlorohydrin should be supplied maximally in the later stages due to its major contribution in chain growth mechanisms.

3) Bisphenol-A must be started in large amount and then must be reduced with time. This is because bisphenol-A takes part actively in polymerization initiation step and its requirement is reduced at the later part. The quantity of addition is observed to prolong for longer time steps for higher values of $M_n$. This happens because a large $M_n$ value is achieved by adding more amount of bisphenol-A in the system. It has been seen that the added bisphenol-A is consumed completely (i.e. not added more than the amount required) in most of the cases.

It is clear from these observations that different polymers (with different $M_n$ and PDI values) must be produced optimally with a different addition pattern of reactants. Although some of these observations can be explained from the chemistry of the process, Figure 2 shows the optimal operating conditions.

To better understand the characteristics of solutions at different parts of the optimized front, we divide the entire front into three groups. As the solutions on optimized front spans $M_n$ from $0.4 \times 10^3$ kg/kg-mole to almost $9.5 \times 10^3$ kg/kg-mole, each region roughly spans $3.0 \times 10^3$ kg/kg-mole in $M_n$ axis: $0.0 - 3.0 \times 10^3$ kg/kg-mole $M_n$ (Group 1), $3.0 - 6.0 \times 10^3$ kg/kg-mole $M_n$ (Group 2) and $6.0 - 9.0 \times 10^3$ kg/kg-mole $M_n$ (Group 3). The representative solution in

each group are shown in Table 1 and the regions for each group is also marked in Figure 1.

**Table 1.** Three representative solutions picked from the optimized front obtained by real-coded NSGA-II in each of the three problems are shown.

| Source | PDI (kg/kg) | $M_n$ (kg/kg-mole) | Reaction time (hr) |
|---|---|---|---|
| Benchmark | 1.61 | 633.2 | 7.00 |
| Problem 1 | | | |
| Group 1 | 1.59 | 926.5 | 7.00 |
| Group 2 | 1.87 | 3186.1 | 7.00 |
| Group 3 | 1.97 | 9507.8 | 7.00 |
| Problem 2 | | | |
| Group 1 | 1.70 | 946.6 | 2.57 |
| Group 2 | 1.90 | 3219.5 | 4.00 |
| Group 3 | 1.99 | 9507.6 | 6.60 |
| Problem 3 | | | |
| Group 1 | 1.61 | 943.71 | 3.80 |
| Group 2 | 1.88 | 3218.02 | 5.17 |
| Group 3 | 1.97 | 9508.45 | 6.98 |

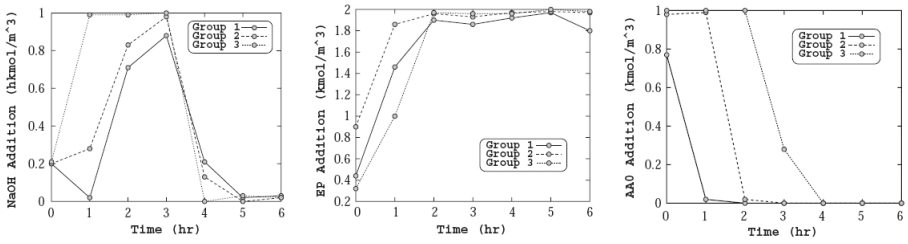


**Fig. 3.** Time-variant additions of NaOH (left), EP (middle), and $AA_0$ (right) are shown for three representative solutions from each group on the optimized front obtained using the real-coded NSGA-II for Problem 1.

The trend in addition of reactants for each group is shown in Figure 3.

Each group has a distinct pattern of adding the three constituents. The information depicted in these figures conveys that there lies a relationship between the solutions in the optimized front and the system under consideration. The relationship can be regarded as the 'blue-print' of the system. Given a set of objectives, certain properties emerge from the system, not arbitrarily, but following some basic properties of the system. This relationship between the property of the system and the solutions of the optimized front would be of tremendous importance to practitioners.

## 5 Discussion on Problems 2 and 3

For brevity, we do not show the obtained front for Problem 2 separately. Instead, we show the front along with the results of Problem 3 obtained using three objectives in Figure 4. It is interesting that the limiting fronts (from problems 1 and 2) lie on the two edges of the three-dimensional front. We deduce the following conclusions from the three-dimensional front:

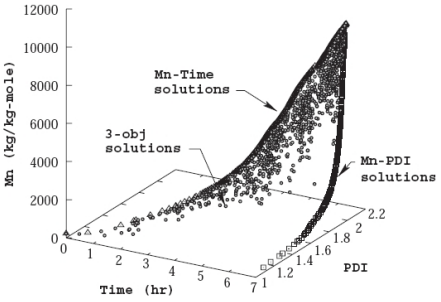


**Fig. 4.** NSGA-II solutions obtained from the three-objective optimization are shown. The fronts obtained in the previous two problems are found to lie on two edges of the obtained three-dimensional front.

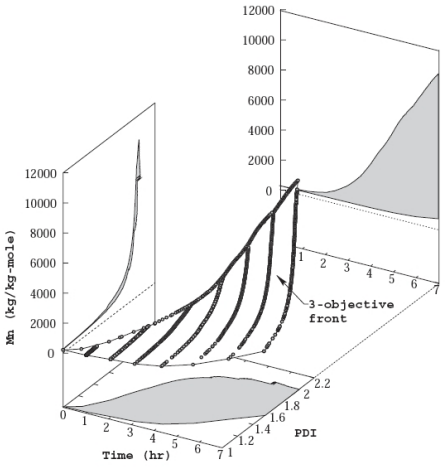


**Fig. 5.** Several optimizations of Problem 1 with $t_{sim}$ values help find the third boundary of true three-dimensional non-dominated front.

1) The three-dimensional non-dominated front is a non-convex front.

2) For low values of $M_n$, polymers can be prepared in much less than 7 hours. Since the reaction time is also minimized in Problem 3, there exists almost no solution requiring as large as 7 hr to produce a polymer having a low $M_n$.

3) For high values of $M_n$, more reaction time is needed. As in the polymerization process, the repeat units get added with the monomer to form a longer chain-length, a polymer having a high value of $M_n$ requires more time to form than a polymer having a low value of $M_n$. But for a desired $M_n$ and PDI combination, one can find a solution requiring smaller than 7 hours to do the job, but occurrence of such a quick operation gets reduced with the requirement of higher and higher $M_n$ values.

4) Finally, for the maximum $M_n$ requirement, there exists only one solution (with $M_n = 10,402.12$ kg/kg-mole), requiring 7 hours (the maximum allowed) of reaction time, but also producing the largest PDI value (1.985). Such is the trade-off often observed in a multi-objective problem and Figure 4 shows many such trade-off solutions producing different $M_n$ and PDI and requiring different amount of reaction time.

5) Another interesting aspect is that for any fixed reaction time, the $M_n$-time optimization (Problem 2) solutions produced the maximum $M_n$ value and there exists no other solution producing a better (smaller) PDI value and an identical $M_n$ value. But, the three-dimensional optimized front provides more information about the trade-off than both two-objective optimized fronts, discussed earlier.

On the three-dimensional optimized front, there seems to be a larger concentration of solutions towards the $M_n$-time front (in other words, there are more solutions requiring a smaller processing time). To understand this trend better, we repeat Problem 1 for different reaction times. We force the reaction time to end at $t_{sim} = 1$ hr, 2 hr and so on, and collect all the obtained optimized solutions. Thereafter, we perform a non-domination check considering all three objectives (maximization of $M_n$, minimization of PDI, and minimization of $t_{sim}$) and the resulting solutions are plotted in Figure 5. An interesting aspect is revealed. For identical PDI values, there exists a smaller reaction time solution outperforming a larger time solution. This feature of the problem produces a *third* boundary on this three-dimensional non-dominated front, thereby showing the complete bounded trade-off surface of interactions. The figure also shows the projection of the three-dimensional trade-off surface on the three two-objective planes. It is clear that although there are some rooms for trade-offs among $M_n$-time and PDI-time combinations, in terms of $M_n$-PDI combinations, there is almost a straightforward trade-off. This fact also indicates that the consideration of minimization of the reaction time is important in this problem to reveal interesting time-saving trade-off solutions. To understand the three-objective interactions further, we consider the PDI-time and $M_n$-time projections (as shown shaded in Figure 5) and plot them again in Figure 6 in the left and right plots, respectively.

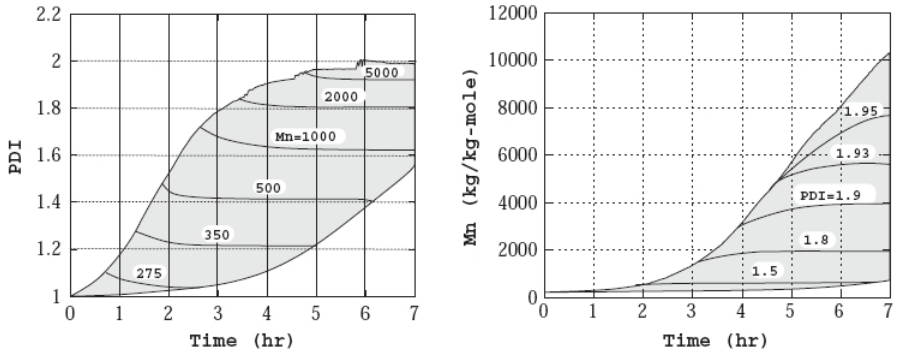


**Fig. 6.** PDI and reaction time interaction (left) and $M_n$ and reaction time interaction (right) reveal interesting properties about the optimal operating conditions of the polymerization problem. In the left figure, $M_n$ is shown in kg/kg-mole.

On the PDI-time plot, we show contours of fixed $M_n$ values. For each contour line, the trade-off between PDI and reaction time is clear. However, what is more

interesting is that the trade-off becomes marginal away from time from the $M_n$-time optimized front (the upper boundary). To achieve a small advantage in the PDI value, a large reaction time is necessary. Since the slope of the three-objective optimized front is quite small at these regions, the NSGA-II has found very few solutions away from the $M_n$-time boundary. It can then be concluded that for fixed $M_n$ requirement, it is better to consider the trade-off solutions close to the $M_n$-time optimized boundary. Another aspect is the rate at which the 'region of optimality' reduces for an increasing $M_n$ value. For example, if a polymer with $M_n$ greater than $5,000$ kg/kg-mole is desired, there does not exist too many options in terms of reaction time. The right plot in Figure 6 shows contour line for fixed values of PDI on the three-objective optimized front. Once again a similar conclusion (about choosing solutions close to the $M_n$-time optimal boundary) can be made for smaller PDI values, for large PDI values (such as PDI=1.95) the trade-off between $M_n$ and reaction time is quite substantial. These two plots can be used to determine a suitable operating condition for a particular application of the epoxy polymerization process.

## 6 Conclusions and Extensions

A well-validated model consisting of a large number of moment-based ordinary differential equations has been utilized for the multi-objective optimization of epoxy polymerization process using an evolutionary algorithm (NSGA-II). The aim of the study has been to extract the discrete addition patterns of the reactants for optimizing various objectives simultaneously (e.g. Problem 1: Maximization of $M_n$ with minimization of PDI, Problem 2: Maximization of $M_n$ with minimization of reaction time and Problem 3: Maximization of $M_n$, minimization of PDI, and minimization of reaction time). All three problems considered here have displayed a non-convex non-dominated front. NSGA-II has been able to find solutions on or near the true non-dominated front of the problems. This has been validated by solving the multi-objective problems using a single-objective preference based optimization method ($\epsilon$-constraint method). The advantage of using the NSGA-II is that it has found multiple (as many as 250) optimized solutions in a single simulation run.

Importantly, the multi-objective optimization of the epoxy polymerization process has led to the discovery of certain operating principles (addition time-pattern of three reactants (NaOH, Epichlorohydrin, and Bisphenol-A)) for all high-performance solutions. The trade-off between the objectives have been clearly characterized by showing and contrasting a representative additive pattern of all three reactants. Such information brings out the 'blue-print' of the optimal operating conditions of a chemical process and are often important in real application in an industry.

## References

1. H. Batzer and S. S. Zahir. Studies in the molecular weight distribution of epoxide resins. *Journal of Applied Polymer Science*, 21:1843, 1977.

2. V. Bhaskar, S. K. Gupta, and A. K. Ray. Applications of multi-objective optimization in chemical engineering. *Reviews in Chemical Engineering*, 16(1):1, 2000.
3. D. Butala, K. Y. Choi, and M. K. H. Fan. Multiobjective dynamic optimization of a semibatch free-radical copolymerization process with interactive cad tools. *Comput. Chem. Eng.*, 12:1115, 1988.
4. S. S. S. Chakravarthy, D. N. Saraf, and S. K. Gupta. Use of genetic algorithm in the optimization of free radical polymerization exhibiting the trommsdorff effect. *J. Appl. Poly. Sci.*, 63:529, 1997.
5. K. Y. Choi and D. N. Butala. An experimental-study of multi-objective dynamic optimization of a semibatch copolymerization process. *Poly. Eng. Sci.*, 31:353, 1991.
6. K. Deb. *Multi-objective optimization using evolutionary algorithms.* Chichester, UK: Wiley, 2001.
7. K. Deb. Unveiling innovative design principles by means of multiple conflicting objectives. *Engineering Optimization*, 35(5):445–470, 2003.
8. K. Deb and R. B. Agrawal. Simulated binary crossover for continuous search space. *Complex Systems*, 9(2):115–148, 1995.
9. K. Deb, S. Agrawal, A. Pratap, and T. Meyarivan. A fast and elitist multi-objective genetic algorithm: NSGA-II. *IEEE Transactions on Evolutionary Computation*, 6(2):182–197, 2002.
10. L. T. Fan, C. S. Landis, and S. A. Patel. *Frontiers in Chemical Reaction Engineering.* New Delhi: Wiley Eastern, 1984.
11. J. N. Farber. Steady state multiobjective optimization of continuous copolymerization reactors. *Poly. Eng. Sci.*, 26:499, 1986.
12. S. Garg and S. K. Gupta. Multiobjective optimization of a free radical bulk polymerization reactor using genetic algorithm. *Macromol. Theor. Simul.*, 8:46, 1999.
13. R. R. Gupta and S. K. Gupta. Multi-objective optimization of an industrial nylon-6 semibatch reactor system using genetic algorithm. *J. Appl. Poly. Sci.*, 73:729, 1999.
14. A. Kumar and S. K. Gupta. *Reaction Engineering of Step Growth Polymerization.* New York: Plenum, 1987.
15. K. Miettinen. *Nonlinear Multiobjective Optimization.* Boston, MA: Kluwer, 1999.
16. K. Mitra, K. Deb, and S. K. Gupta. Multi-objective dynamic optimization of an industrial nylon 6 semibatch reactor using genetic algorithm. *J. Appl. Poly. Sci.*, 69:69, 1998.
17. S. Raha, S. Majumdar, and K. Mitra. Effect of caustic addition in epoxy polymerization process: A single and multiobjective evolutionary approach. *Macromolecular Theory and Simulations*, in press.
18. R. Sareen and S. K. Gupta. Multiobjective optimization of an industrial semibatch nylon 6 reactor. *J. Appl. Poly. Sci.*, 58:2357, 1995.
19. N. Srinivas and K. Deb. Multi-objective function optimization using non-dominated sorting genetic algorithms. *Evolutionary Computation Journal*, 2(3):221–248, 1994.
20. A. Tsoukas, M. V. Tirrell, and G. Stephanopoulos. Multi-objective dynamic optimization of semibatch copolymerization reactors. *Chem. Eng. Sci.*, 37:1785, 1982.
21. R. M. Wajge and S. K. Gupta. Multiobjective dynamic optimization for a nonvaporizing nylon-6 batch reactor. *Poly. Eng. Sci.*, 34:1161, 1994.